Journal of Physics D: Applied
Physics

PAPER • OPEN ACCESS

Characteristics of parametric spin waves in rectangular magnonic blocks

OPEN ACCESS
IOP Publishing

Journal of Physics D: Applied Physics

J. Phys. D: Appl. Phys. **54** (2021) 365001 (8pp)

https://doi.org/10.1088/1361-6463/ac0ad2

Characteristics of parametric spin waves in rectangular magnonic blocks

S Hwang[1,2], Seungha Yoon[2], B R Kim[1], S H Han[3] and B K Cho[1,*]

[1] School of Materials Science and Engineering, Gwangju Institute of Science and Technology (GIST), Gwangju 61005, Republic of Korea
[2] Smart Energy & Nano Photonics Group, Korea Institute of Industrial Technology, Gwangju 61012, Republic of Korea
[3] Division of Navigation Science, Mokpo National Maritime University, Mokpo 58628, Republic of Korea

E-mail: chobk@gist.ac.kr

Received 20 January 2021, revised 17 May 2021
Accepted for publication 11 June 2021
Published 24 June 2021

Abstract

The characteristics of parametric spin-wave pumping are investigated in three rectangular permalloy blocks with in-plane aspect ratios of 12, 6, and 4. Micro-Brillouin light scattering (BLS) spectroscopy is utilized to detect the intrinsic properties of excited spin waves under various excitation conditions of an external magnetic field and microwave power. Based on the theoretical dispersion relation and BLS intensity and its spatial profile, the parametric spin wave with a frequency of $f_{sw} = 5.6$ GHz is found to be excited in fundamental mode in a block of largest aspect ratio while the other block have higher-order or edge-localized modes along the width direction. The data shows that the nature of spin waves is quite sensitive on the conditions of sample geometry, applied field and microwave power. Thus, with the appropriate combination of the three parameters, it would be possible to control the nature of spin wave in each block simultaneously, which increase the blocks' potential in magnonic applications, such as spin-logic and interferometer.

Supplementary material for this article is available online

Keywords: parallel parametric pumping, spin wave, magnonics, rectangular block, threshold characteristics

(Some figures may appear in colour only in the online journal)

1. Introduction

Over the last few decades, the field of so-called magnonics [1–4], where spin waves are utilized as information carriers, has been studied intensively. One attractive application of magnonics is its use in low-loss and ultra-fast non-volatile logic devices. To improve the feasibility of magnonic logic systems, there are several issues to be addressed, one of which is spin-wave excitation for efficient signal transmission. For data processing, spin waves must be transmitted to the manipulation area, while overcoming the signal loss due to spin-wave damping. To achieve low-loss transmission, the study of excitation techniques suitable for magnetic systems is essential.

The coupling of magnetization m with a microwave field H_{mw}, induced by a microwave current, is the most common spin-wave excitation method. There are two representative excitation mechanisms, depending on the angle between H_{mw} and the external field H_{ex}. In linear excitation, i.e. force excitation, the orientation of H_{mw} is perpendicular to H_{ex}, and the spin-wave frequency is identical to that of H_{mw} [5]. In force excitation, an antenna that guides the microwave current should be situated across a magnetic element. Both the antenna width and the microwave-field uniformity limit

* Author to whom any correspondence should be addressed.

the characteristics of the excited spin wave [6, 7]. With this structural restriction, only a spatially symmetric spin wave with a long wavelength, in principle, can be excited. To achieve short wavelength (≈50 nm), additional hetero-structure, rather than a simple waveguide, should be introduced in the forced excitation [8]. In contrast, parallel parametric pumping [9], where H_{mw} is applied parallel to H_{ex}, induces nonlinear excitation, in which the microwave photon with frequency f_p splits into two spin waves with opposite wave vectors, both with frequency $f_p/2$.

In a parametric process, pumped spin wave has a much larger amplitude than the spin wave created by force excitation, and a wide range of wave vectors from dipolar- to exchange-dominant can be excited when the microwave power P exceeds a certain threshold value P_{th} [10]. The threshold is determined by the damping parameter of the magnetic material and the ellipticity of magnetic precession-i.e. the ratio of the in-plane magnetization components. That is, low damping and high ellipticity enhance the parametric pumping efficiency [11]. Another pumping condition is that the half of f_p should be larger than the minimum frequency f_{min} of the spin-wave band in the corresponding magnetic structure [12]. On the other hand, it should be mentioned that there can be also the exceptional case, such as threshold process involved off-resonant driven spin wave mode with wave vectors near $k = 0$ in a nanostructure [13]. In this case, the spin waves with the slightly lower frequency than f_{min} can be excited. The conversion of input microwaves of frequency f_p in a parametric process can be controlled by adjusting the dispersion relation of the excited wave vectors, which depends on the magnitude of H_{ex}. Thus, microwave power and frequency, and the magnitude of the external field are the key parameters in modulating the parametric process to produce various wave modes.

Another issue is the manipulation of spin waves for logical operation. For example, various types of magnonic crystals (MCs), as components in logic devices, have been studied [14–17]. MCs, comprising periodically patterned magnetic media, allow the construction of artificially tailored band structures and, consequently, the modulated magnetic properties required by spin-wave waveguides [18, 19], filters [20, 21], and multiplexers [22, 23]. In particular, a width-modulated structure [24–26] is representative of MC structure, and utilizes wave-reflection properties in conjunction with the difference of the dispersion relation due to variation in the width w of a unit block. Thus, it is necessary to better understand the dispersion relations of MC blocks for the comprehensive interpretation of signal processing. The size effect, as well as difference of dispersion relation, also affects the threshold property of parametric excitation as the concentration of pumping energy is more efficient in a smaller volume [27, 28].

In this paper, parametric pumping characteristics are investigated in three rectangular blocks with identical length and thickness, but various widths, i.e. the in-plane aspect ratios (length/width) of 12, 6, and 4. The pumping threshold and spin wave properties are studied using a micro-Brillouin light scattering (μ-BLS) spectrum and its spatial profiles, with a combination of three control parameters: w, H_{ex}, and P. Analysis of the data in terms of the calculated dispersion relation reveals that the pumping efficiency and nature of spin waves are sensitive to size variation in magnetic blocks.

2. Experimental details

Spectroscopic measurement is carried out using a μ-BLS system, interfaced with a programmable computer [29]. The μ-BLS system possesses a microscope objective with a high magnification (100×) and large numerical aperture (0.75) to obtain a beam spot size of approximately 250 nm in diameter, which significantly enhances the lateral resolution limit. The incident beam, generated by a 532 nm-wavelength, diode-pumped solid laser, is focused on a specific position in the magnonic block through the objective lens. The sample is located on an x–y–z piezoelectric stage for spatial scanning at the nanometer scale to plot an intensity map of the spin-wave mode. Light scattered from spin waves in the permalloy (Py) blocks passes through a (3 + 3) pass tandem Fabry–Perot interferometer to obtain a frequency-domain spectrum. The laser intensity in our experiment is reduced to less than 1 mW to minimize possible thermal effects.

Figure 1(a) shows the schematic geometry of the system setup. Rectangular Py blocks of 30 nm thickness, 6 μm length (l), and various widths (w) are fabricated using e-beam lithography and magnetron sputtering on a Cu antenna of 200 nm thickness. The clear SEM image is shown in the inset. Each block is named, depending on its width: A, B, and C: 500, 1000, and 1500 nm width, respectively. A 30 nm thick SiO_2 layer is deposited between the blocks and antenna for insulation. The external field is applied along the width direction. The microwave current for parametric pumping has a 11.2 GHz pulse over a duration of 500 ns, with a repetition time of 1 μs to prevent thermal degradation due to Joule heating. The dynamic field, induced by the microwave current, should be parallel to the external field direction. In addition, the micromagnetic simulation, OOMMF [30], was performed to ensure the existence of the magnetization component parallel to the microwave field. The structural geometry for the simulation is same as the thickness and in-plane aspect ratio of block A. It shows that the magnetization, parallel to the excitation field, is aligned even with the lowest applied field, 570 Oe, in our experiment (see the supplementary information, figure S-1 (available online at stacks.iop.org/JPD/54/365001/mmedia)). Accordingly, our experimental geometry satisfies the condition for parallel parametric pumping. It should be mentioned that we expect energy loss in this system because the Cu micro-stripe antenna serves as a kind of waveguide. So, it would be possible to excite the spin waves with less power than that in this study once elegant wave guides are adopted in system. The measurements for the individual block show the same features, presented in this manuscript.

3. Results and discussion

It is well known that parametric excitation is closely related to the dispersion relation of the corresponding spin-wave

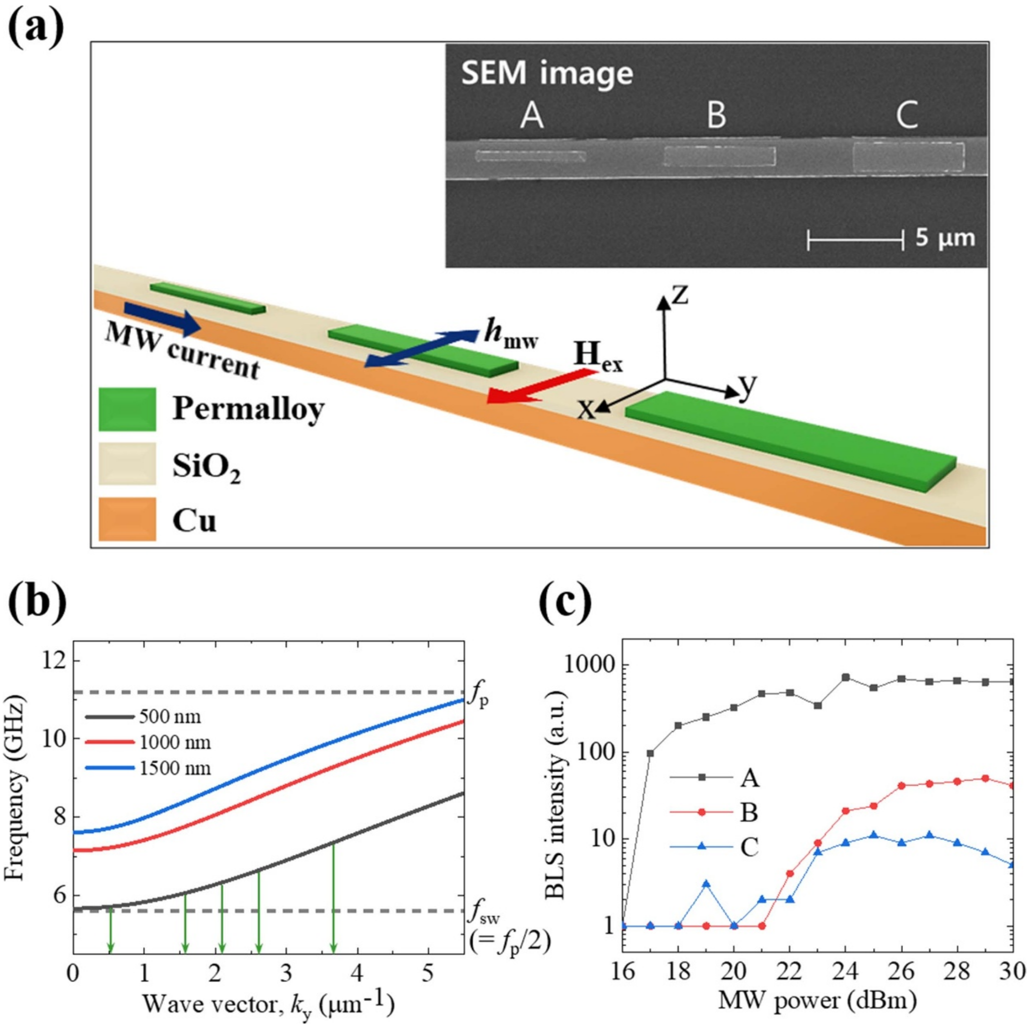

Figure 1. (a) Schematic geometry of experimental setup for parametric pumping. The permalloy blocks are deposited on a Cu antenna, and SiO_2 is used for insulation. The microwave current flows along the y-axis in the Cu antenna and generates a dynamic field (h_{mw}). The external field (H_{ex}) is applied along the z-axis. The inset is an SEM image of the top surface of the setup. (b) The dispersion curves with $H_{ex} = 800$ Oe correspond to the blocks: A (500 nm width), B (1000 nm width), and C (1500 nm width). (c) BLS spectrum intensity with $H_{ex} = 800$ Oe as a function of microwave power for the three blocks.

system. A direct comparison between the experimental data and the calculated dispersion relation was carried out to better understand the parametric spin-wave transition [31–33]. In this study, we performed an analytical approximation to obtain the dispersion relation using the well-established equation for a wire with the same dimension as each block [34, 35]

$$\omega_n = \left[\left(\omega_H^n + \lambda_{ex}\omega_M k^2\right)\left(\omega_H^n + {\lambda_{ex}}^2\omega_M k^2 + \omega_M F(kL)\right)\right]^{1/2}, \quad (1)$$

where $\omega_H^n = \omega_H + \omega_M N_{xx}(x), \omega_H = \gamma H_{ex}, \omega_M = 4\pi\gamma M_s, k^2 = k_y^2 + k_{nx}^2$ with $k_{nx} = \frac{n\pi}{w}$ $(n = 1, 2, 3\cdots)$, $\lambda_{ex} = \sqrt{\frac{A}{2\pi M_s^2}}$, and $F(kL)$ is a quantized matrix element of the dipole-dipole interaction. The n denotes the antinode number across the width in the width-quantized mode, which has the characteristics of the quasi-uniform mode resonating through the width of the block [36, 37]. The width-quantized mode Standard parameter values for permalloy [38, 39] are the following: the gyromagnetic ratio $\gamma/2\pi = 28$ GHz/T, saturation magnetization $M_s = 860$ emu cm^{-3}, and the exchange constant $A = 1.3 \times 10^{-6}$ erg cm^{-1}. $F(kL)$ can be calculated from the following equation using the above defined quantities [40].

$$F(kL) = 1 + P(kL)[1 - P(kL)]\left(\frac{\omega_M}{\omega_H^n + {\lambda_{ex}}^2\omega_M k^2}\right) \times \left(\frac{k_y^2}{k^2}\right) - P(kL)\left(\frac{k_{nx}^2}{k^2}\right), \quad (2)$$

with $\mathrm{P}(kL) = 1 - \frac{1-\exp(kL)}{kL}$.

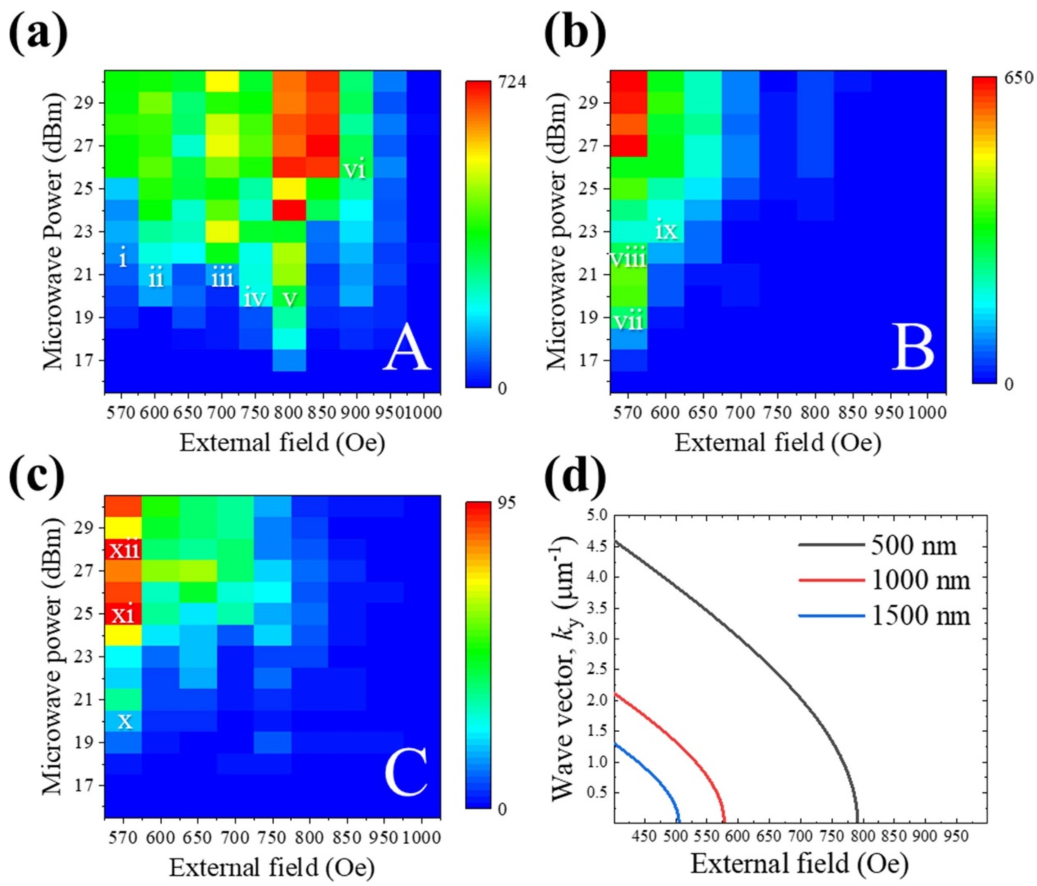

Figure 2. (a)–(c) μ-BLS spectrum intensity plot, which shows the threshold characteristics of blocks A, B, and C. The spectrum intensity is taken at the center of the blocks. The external field and microwave power are applied in steps of $\Delta H_{\mathrm{ex}} = 50$ Oe and $\Delta P = 1$ dBm, respectively. (d) Analytical calculation of the field dependence of the longitudinal wave vector k_y in the unit of 1/ μm for a fixed frequency of $f_{\mathrm{sw}} = 5.6$ GHz in the 500, 1000, and 1500 nm blocks.

The effective demagnetization factor, $N_{xx}(x)$, of a width-quantized mode in a transversely magnetized wire is calculated analytically using the following equation [36, 41]:

$$N_{xx}(x) = \frac{1}{\pi}\left[\arctan\left(\frac{t}{2x+w}\right) - \arctan\left(\frac{t}{2x-w}\right)\right], \quad (3)$$

for a thickness of $t = 30$ μm. The demagnetization factor value at the center of the wire is used in our calculation. The dispersion curves for blocks of various widths, 500, 1000, and 1500 nm, are plotted in figure 1(b). The dispersion curves of the $n = 1$ width-quantized mode under $H_{\mathrm{ex}} = 800$ Oe are found to shift to higher frequencies as width increases. Because the parametric pumping process generates the spin wave with frequency f_{sw}, which should be half the pumping frequency f_{p} (=11.2 GHz), the dispersion curves indicate that parametric pumping occurs only in the 500 nm width block where the spin wave mode exists within f_{sw} (=5.6 GHz). The μ-BLS spectrum at a frequency of $f_{\mathrm{sw}} = 5.6$ GHz is measured at the center of each block, and spectral intensity as a function of microwave power is plotted in figure 1(c). An excitation spectrum is clearly evident in the 500 nm block, while much less one in high power is observed in the other blocks; this is consistent with the analytical dispersion calculation in figure 1(b).

In order to study the field effect on parametric excitation at $f_{\mathrm{p}} = 11.2$ GHz, the μ-BLS spectrum are measured and the spectrum intensity map is plotted in terms of microwave power and field for the three blocks in figure 2. The applied external field is in the range 570 Oe $\leq H \leq$ 1000 Oe, with a step of 50 Oe, and the microwave power ranges from 16 to 30 dBm, with a 1 dBm step. The field of 570 Oe is the measurement system limit. For block A in figure 2(a), the lowest threshold power, where the BLS signal increases exponentially [31], occurs at a field of $H_{\mathrm{ex}} = 800$ Oe, as expected in the dispersion relation in figure 1(b). When the field varies, the threshold pumping power increases in either higher or lower fields than $H_{\mathrm{ex}} = 800$ Oe, and higher fields induce steeper increases in threshold power than lower fields, resulting in an asymmetric butterfly curve. In contrast, the threshold characteristics of block B (figure 2(b)) and C (figure 2(c)) show that threshold power is lowest at $H_{\mathrm{ex}} = 570$ Oe and increases with increasing field strength.

The field dependence of the longitudinal wave vector k_y is calculated using the wire approximation and plotted for the three blocks in figure 2(d)—the curves are for the width-quantized mode ($n = 1$) of the spin wave, with a fixed frequency of $f_{\mathrm{sw}} = 5.6$ GHz. Because the wave vector for block A increases as the field decreases below $H_{\mathrm{ex}} = 800$ Oe, the

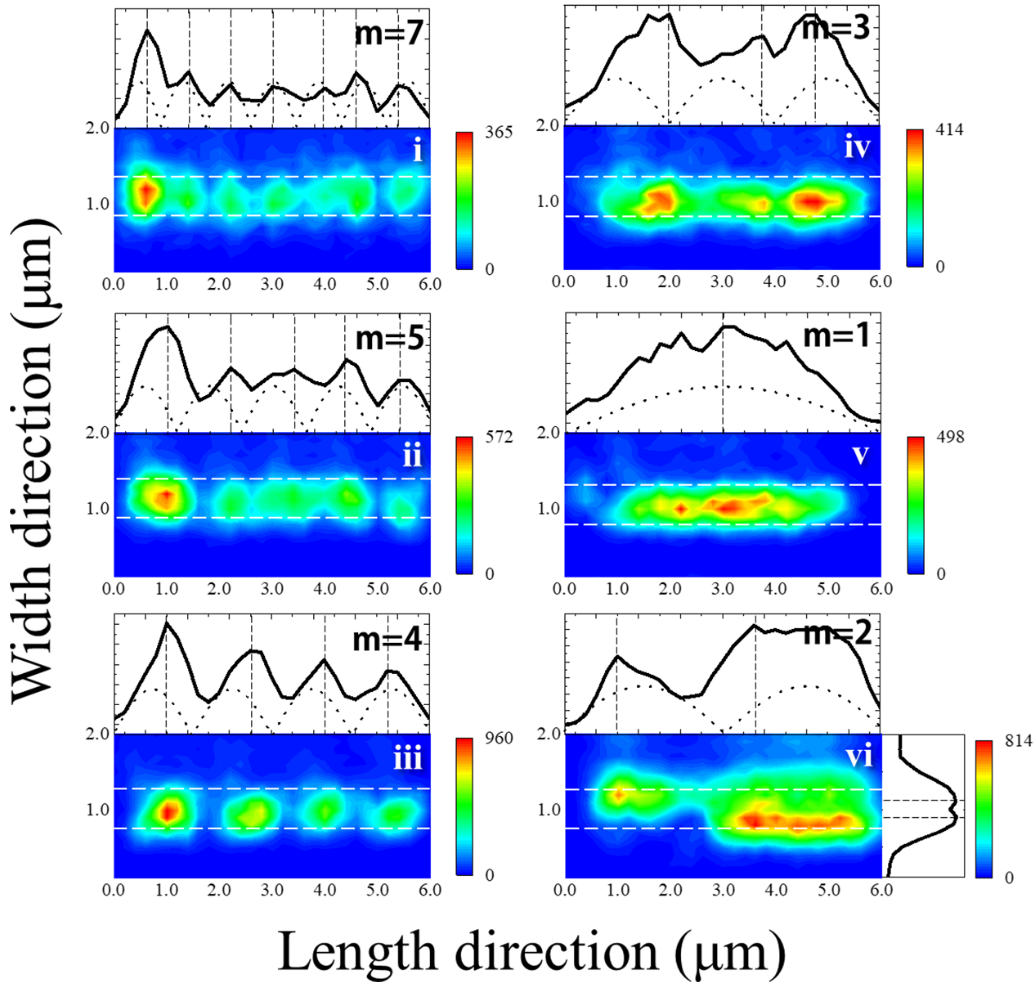

Figure 3. Spatial profiles of block A under excitation conditions i–vi in figure 2(a). Real line in the upper panel (and right panel) represents the integrated spin-wave intensity, and the dotted-line represents the calculated magnetization distribution of the length-quantized mode. m is the antinode numbers in the length-directions.

butterfly curve in the low-field regime in figure 2(a) is to be expected. In high fields of H_{ex} > 800 Oe, a spin wave with an $n = 1$ mode is not excited, but those with higher-order, width-quantized modes ($n > 1$) are. In addition, an edge-localized spin wave is possible in high fields. The large wave vector in a spin wave with antinodes ($n > 1$) reduces the ellipticity of excited spin waves, eventually significantly decreasing the coupling efficiency of the microwave field H_{mw} with the existing spin wave [42]. This is why the threshold characteristics curve in figure 2(a) is asymmetric in the high-field regime. Thus, we surmise that spin waves with higher-order, width-quantized modes, as well as the $n = 1$ mode, with various k_y would be excited by parametric pumping, depending on the external field H_{ex} in block A. The field dependence of the wave vectors for blocks B and C shows that the $n = 1$ mode spin wave is not likely to be excited in fields of $H_{ex} \geqslant 570$ Oe. This means that the increase in threshold power in figures 2(b) and (c) is due to the excitation of higher-order modes.

Figures 3 and 4 show spatial profiles of the excited spin waves. To obtain spatial profiles, space-resolved μ-BLS is performed on the spots of $(x \times y) = (35 \times 25)$ with measurement intervals of 200 nm and 100 nm along the x-axis and y-axis, respectively. The six profiles in figure 3 are obtained from the top surface of block A, with pumping conditions specified by roman numerals i–iv in figure 2(a). For the precise observation of a mode transition, which depends on the field, the pumping condition of selected profiles is near the threshold power P_{th}. This is because large pumping energies above P_{th} induce competition between various dipole-dominant modes and, eventually, flow into fundamental mode with the lowest value of k_y [28]. For condition v, where we expect an $n = 1$ mode spin wave, the lowest k_y value and the lowest threshold power, the profile shows the intensity distribution of $n = 1$ mode along the width-direction. In addition, the intensity distribution along the length direction is plotted (real line) together with the calculated magnetization distribution using $\cos(k_m y)$ and $\sin(k_m y)$ (dotted line) for symmetric and antisymmetric distribution, respectively, in upper panel of the spatial profile [43]. It shows the fundamental spin wave with one antinode ($m = 1$) along the length direction, which is consistent with the calculated magnetization. Under conditions i–iv, although the spatially resolved μ-BLS intensities are of the n = 1 mode along the width direction, the antinode

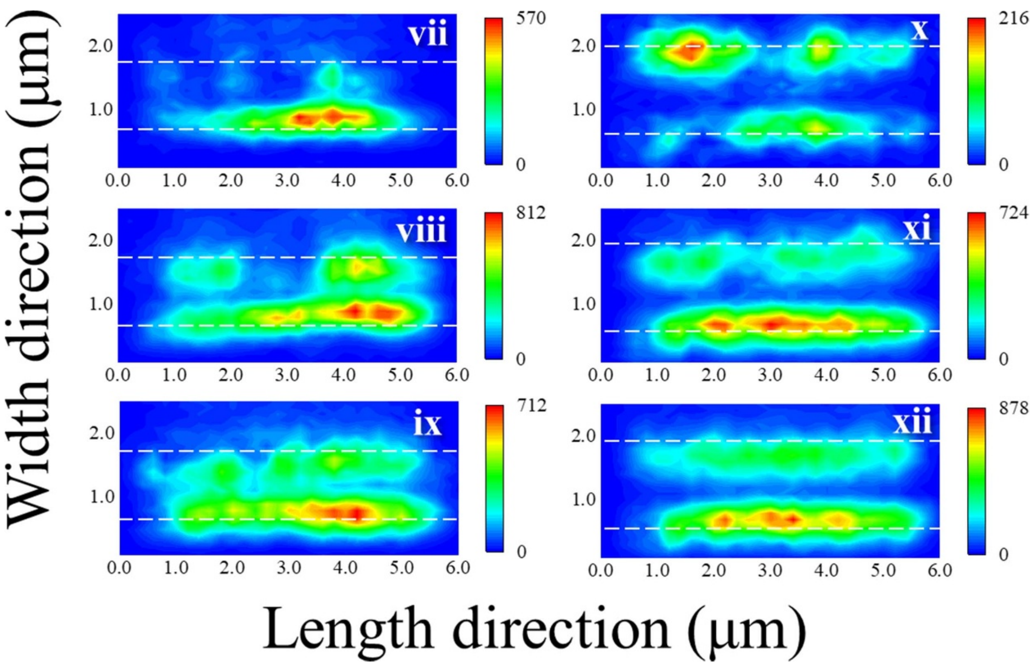

Figure 4. Spatial profiles of blocks B (left column) and C (right column) under excitation conditions vii–xii in figures 2(b) and (c).

number of spin waves along the length direction increases; this means the quantized k_y value increases as the field decreases, shown in figure 2(d). The variation in intensity is qualitatively consistent with the calculated magnetization under conditions i–iv. The values of the length-quantized wave vector k_m ($= \frac{m\pi}{l}$, $m = 1-7$), indicated by green arrows in figure 1(b), are within the field range of 500 Oe $\leqslant H_{ex} \leqslant$ 800 Oe, in which the measurement was performed. Because of the quantization effect along both the width and length directions, the measurement profile represents the standing spin wave. In contrast, under condition vi, where we expect a higher-order width-quantized mode, the profile shows the spin wave of the non-fundamental mode along both the width and length directions as depicted with real lines in the upper and right panels. Because the analytic dispersion curve calculated by equation (1) of $n = 2$ mode with $H = 900$ Oe indicates that the minimum frequency for parametric pumping should be larger than $f_{sw} = 6.3$ GHz, the spin wave under condition vi is likely of edge-localized mode, rather than $n = 2$ mode.

Figure 4 shows the spatial profiles of blocks B and C under the various excitation conditions specified in figures 2(b) and (c): the conditions, vii, viii, and ix, in left (block B) and, x, xi, and xii, in right (block C). All profiles show the characteristics of non-fundamental modes, i.e. spin wave with a higher-order width-quantized mode (likely $n = 2$) or edge mode, which is consistent with our expectation from the wave vector variation in the blocks, depicted in figure 2(d). Field-dependence of the longitudinal wave vector k_y of $n = 2$ mode at $f_{sw} = 5.6$ GHz for blocks of B and C shows that the mode can exist below $H = 586$ and 512 Oe, respectively (see the supplementary information, figure S-2). Thus, it is possible for the profiles in vii and viii conditions to be of $n = 2$ mode and other profiles should be of edge-localized mode. But it is hard to distinguish the two modes in this study. It is also noted that the spatial profiles in vi condition in figures 3 and 4 show noticeable asymmetry in BLS signal along both the width and length directions. Because the asymmetric distribution is observed in high power region regardless of sample geometry, it might be from interference between the propagating waves with different modes. It is interesting to have BLS intensity data from the Anti-stokes peak to discuss the interference scenario (BLS intensity in this manuscript is measured from the Stokes peak). In addition, in order to have clues on the mode transition between the second waveguide mode and edge mode, it is necessary to perform further experiments with the applied field in a finer step (in progress).

The threshold characteristics of blocks A and B in figure 2 are plotted together in figure 5. The area enclosed by a black dashed line indicates the H_{ex} versus P space, where parametric pumping occurs simultaneously in both blocks A and B. Red and blue in the area indicate the excitation conditions in which the spin wave in blocks A and B dominates, respectively. Moreover, although blocks A and B have dimensions conducive to parametric pumping, the intrinsic nature of the excited spin wave in one block is different from that in the other block. That is, the spin wave from block A has the $n = 1$ mode, while the wave from block B has higher-order modes along the width direction. Threshold conditions for parametric pumping that occur only in A or B are also confirmed in the area outside the black dashed-line. It might be useful to take advantage of such simultaneous and sole excitation conditions for magnonic logic devices. For example, assuming a width transition structure, combining magnetic blocks A and B, it is possible to make spin waves flow from A (B) to B (A) to control the spin-wave propagation direction using appropriate threshold conditions, where parametric pumping

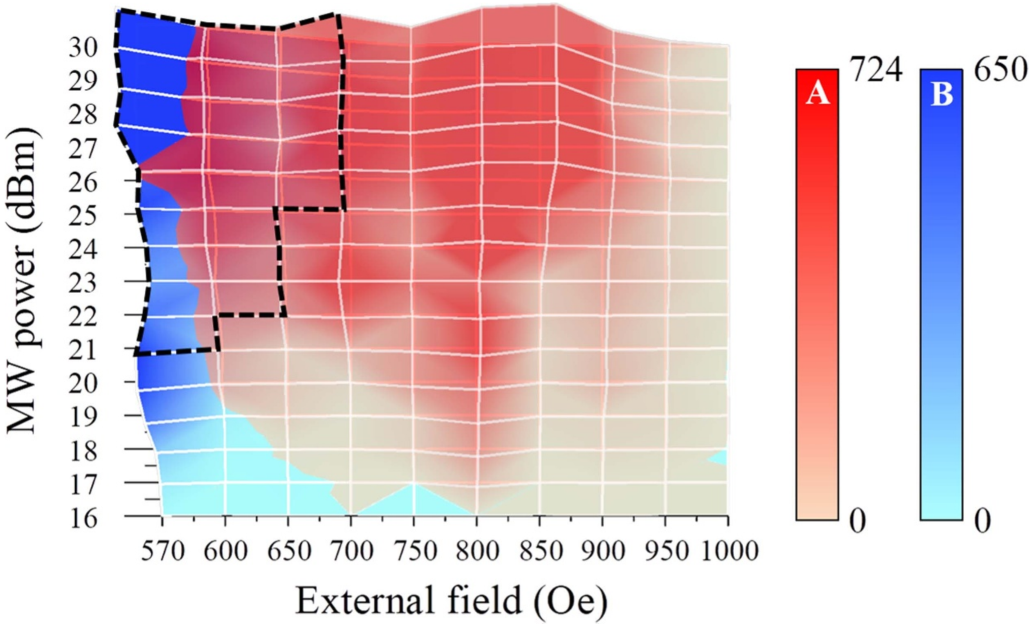

Figure 5. μ-BLS intensity map for blocks A and B. The area enclosed by dashed line indicates the pumping conditions for the simultaneous excitation of spin waves in blocks A and B. The blue and red in the area represent the spin waves, which are dominant in blocks B and A, respectively.

occurs only in A (B). Another example is a structure consisting of three blocks. By adjusting H_{ex} and P conditions, parametric spin-wave pumping can be made to occur only in two blocks on either side of the center block. In this case, the center block would act as a new-concept of interferometer, which could replace the conventional Mach–Zender-type interferometer [44, 45]. To realize the prototypes of magnonic logic and interferometer, further study on the structure of magnetic blocks, design of system, and, most importantly, inductive detection of propagating wave, etc should be done.

4. Summary

We study the characteristics of parametric spin-wave pumping in wire-type magnetic blocks with a fixed length (6 μm), thickness (30 nm), and various widths. For a block of 500 nm width, parametric spin waves of both fundamental and higher-order width-quantized modes are excited at a fixed frequency, f_{sw} = 5.6 GHz, in a field range of 570 Oe $\leqslant H \leqslant$ 1000 Oe. In addition, the field is found to be an effective parameter in adjusting spin-wave modes in length quantization, as well as in width quantization. As block width increases (1000 and 1500 nm), the excitation power is found to increase in a small field window near $H = 570$ Oe. The spatial profile of the μ-BLS spectrum shows that no fundamental mode is excited, but only higher-order or edge modes along the width. These features in parametric pumping are consistent with an analytical calculation of wave vector variation using the parameters of size and field. This means that the parametric excitation can be manipulated depending on the parameters of not only microwave power and applied field, but also of block geometry, e.g. in-plane aspect ratio, in the magnetic blocks. Thus, the results open possibility that magnonic devices, which contain series of magnetic blocks, can be developed for a new concept of spin-based electronics.

Author contributions

B K C and S H conceived the project idea and planned the experiment. S H fabricated samples and performed the analytical calculation. S H and B R K performed the measurement. S H, S H Y, S H H and B K C analyzed the data. B K C led the work and wrote the manuscript with S H All authors discussed the results and commented on the manuscript.

Data availability statement

The data that support the findings of this study are available upon reasonable request from the authors.

Acknowledgments

This work was supported by GIST Research Institute (GRI) grant funded by the GIST in 2021, by the Korea Institute of Industrial Technology (KITECH), and by National Research Foundation of Korea (NRF) grant funded by the Ministry of Science and ICT (No. NRF-2017R1A2B2008538 and NRF-2018R1A2B6005183).

ORCID iDs

S Hwang https://orcid.org/0000-0002-1983-7615
B R Kim https://orcid.org/0000-0001-7420-969X

References

[1] Kruglyak V and Hicken R 2006 *J. Magn. Magn. Mater.* **306** 191–4
[2] Neusser S and Grundler D 2009 *Adv. Mater.* **21** 2927–32
[3] Kruglyak V, Demokritov S and Grundler D 2010 *J. Phys. D: Appl. Phys.* **43** 264001
[4] Serga A, Chumak A and Hillebrands B 2010 *J. Phys. D: Appl. Phys.* **43** 264002
[5] Kittel C 1948 *Phys. Rev.* **73** 155–61
[6] Ganguly A K and Webb D C 1975 *IEEE Trans. Microwave Theory Tech.* **23** 998–1006
[7] Demidov V E, Demokritov S O, Rott K, Krzysteczko P and Reiss G 2008 *Phys. Rev.* B **77** 064406
[8] Liu C P *et al* 2018 *Nat. Commun.* **9** 738
[9] Schlömann E, Green J and Milano U 1960 *J. Appl. Phys.* **31** S386–95
[10] Sandweg C W, Kajiwara Y, Chumak A V, Serga A A, Vasyuchka V I, Jungfleisch M B, Saitoh E and Hillebrands B 2011 *Phys. Rev. Lett.* **106** 216601
[11] Bracher T, Pirro P and Hillebrands B 2017 *Phys. Rep.* **699** 1–34
[12] Okano G and Nozaki Y 2019 *Phys. Rev.* B **100** 104424
[13] Yarbrough P M and Livesey K L 2018 *J. Appl. Phys.* **123** 043904
[14] Al-Wahsh H, Akjouj A, Djafari-Rouhani B and Dobrzynski L 2011 *Surf. Sci. Rep.* **66** 29–75
[15] Lenk B, Ulrichs H, Garbs F and Münzenberg M 2011 *Phys. Rep.* **507** 107–36
[16] Chumak A V, Serga A A and Hillebrands B 2017 *J. Phys. D: Appl. Phys.* **50** 244001
[17] Zakeri K 2020 *J. Phys.-Condens Matter* **32** 363001
[18] Kłos J W, Kumar D, Krawczyk M and Barman A 2013 *Sci. Rep.* **3** 2444
[19] Schwarze T and Grundler D 2013 *Appl. Phys. Lett.* **102** 222412
[20] Chumak A V, Serga A A, Hillebrands B and Kostylev M P 2008 *Appl. Phys. Lett.* **93** 022508
[21] Sadovnikov A V, Gubanov V A, Sheshukova S E, Sharaevskii Y P and Nikitov S A 2018 *Phys. Rev. Appl.* **9** 051002
[22] Morozova M A, Grishin S V, Sadovnikov A V, Romanenko D V, Sharaevskii Y P and Nikitov S A 2015 *Appl. Phys. Lett.* **107** 242402
[23] Frey P *et al* 2020 *Commun. Phys.* **3** 17
[24] Chumak A V *et al* 2009 *Appl. Phys. Lett.* **95** 262508
[25] Lee K S, Han D S and Kim S K 2009 *Phys. Rev. Lett.* **102** 127202
[26] Nikitin A A, Ustinov A B, Semenov A A, Chumak A V, Serga A A, Vasyuchka V I, Lähderanta E, Kalinikos B A and Hillebrands B 2015 *Appl. Phys. Lett.* **106** 102405
[27] Demidov V E, Ulrichs H, Demokritov S O and Urazhdin S 2011 *Phys. Rev.* B **83** 020404(R)
[28] Ulrichs H, Demidov V E, Demokritov S O and Urazhdin S 2011 *Phys. Rev.* B **84** 094401
[29] Demokritov S O and Demidov V E 2008 *IEEE Trans. Magn.* **44** 6–12
[30] Donahue M J and Porter D G 1999 OOMMF user's guide, version 1.0 (Gaithersburg, MD: NIST)
[31] Bracher T, Pirro P, Obry B, Leven B, Serga A A and Hillebrands B 2011 *Appl. Phys. Lett.* **99** 162501
[32] Bracher T, Pirro P, Serga A A and Hillebrands B 2013 *Appl. Phys. Lett.* **103** 142415
[33] Bracher T, Pirro P, Heussner F, Serga A A and Hillebrands B 2014 *Appl. Phys. Lett.* **104** 092418
[34] Kalinikos B A and Slavin A N 1986 *J. Phys. C: Solid State Phys.* **19** 7013
[35] Demokritov S O, Hillebrands B and Slavin A N 2001 *Phys. Rep.* **348** 441–89
[36] Bayer C *et al* 2005 *Phys. Rev.* B **72** 064427
[37] Wang Q *et al* 2019 *Phys. Rev. Lett.* **122** 247202
[38] Ulrichs H, Demidov V E and Demokritov S O 2014 *Appl. Phys. Lett.* **104** 042407
[39] Kwak W Y, Yoon S, Kwon J H, Grunberg P and Cho B K 2016 *J. Appl. Phys.* **119** 023904
[40] Guslienko K Y, Chantrell R W and Slavin A N 2003 *Phys. Rev.* B **68** 024422
[41] Joseph R I and Schlömann E 1965 *J. Appl. Phys.* **36** 1579–93
[42] Gurevich A G and Melkov G A 1996 Magnetization Oscillations and Waves (New York: CRC)
[43] Guslienko K Y, Demokritov S O, Hillebrands B and Slavin A N 2002 *Phys. Rev.* B **66** 132402
[44] Lee K S and Kim S K 2008 *J. Appl. Phys.* **104** 053909
[45] Schneider T, Serga A A, Leven B, Hillebrands B, Stamps R L and Kostylev M P 2008 *Appl. Phys. Lett.* **92** 022505